



## Migration of vacancies, He interstitials and He-vacancy clusters at grain boundaries in $\alpha$ -Fe

F. Gao\*, H.L. Heinisch, R.J. Kurtz

Pacific Northwest National Laboratory, Richland, WA 99352, USA

### ARTICLE INFO

PACS:  
D0300  
G0200  
I0200  
T0100

### ABSTRACT

The dimer method for searching transition states has been used to systematically study possible migration paths of vacancies, He interstitials and He-vacancy (He/V) clusters at  $\Sigma 11\langle 110 \rangle$  {323} and  $\Sigma 3\langle 110 \rangle$  {111} grain boundaries (GBs) in  $\alpha$ -Fe. Vacancies trapped at the GBs diffuse along the GBs with migration energies much less than that within the perfect crystal. Long-time dynamics simulations of diffusion pathways reveal that vacancies migrate one-dimensionally along specific directions in both GBs: directly along close-packed rows in the  $\Sigma 3$  GB, and in zigzag paths within the  $\Sigma 11$  GB. Also, dimer saddle point searches show that He interstitials can diffuse along the GBs with migration energies of 0.4–0.5 eV, similar to those of individual vacancies at the GBs, and the corresponding mechanisms are determined. The rate-controlling activation energy for migration of a He-divacancy cluster in the GBs determined using the dimer method is about 0.9 eV. This is comparable to the migration energy for a He-divacancy cluster in bulk  $\alpha$ -Fe.

© 2009 Elsevier B.V. All rights reserved.

### 1. Introduction

For fusion materials development, one of the most important issues is the high rate of helium production by (n, $\alpha$ ) reactions. The interactions of these He impurities with microstructural features, such as dislocations and grain boundaries (GBs), can result in adverse effects on mechanical properties of metals and alloys. Particularly, high helium concentrations can lead to the formation of helium bubbles that enhance void swelling and cause embrittlement by intergranular fracture along GBs [1–3]. Thus, the formation of He bubbles both in bulk and at GBs remains one of the most important aspects in nuclear fusion technology. A detailed knowledge of He diffusion in both the bulk and at GBs, including the mobility of small helium-vacancy clusters and the nucleation of helium bubbles, is extremely important to quantitatively understand the fate of He atoms with respect to the microstructural features with which they interact. In addition, it is realized that the transportation of defects within various microstructures may be important for the understanding of microstructural evolution under irradiation, especially if their migration behavior is significantly different from that in the bulk.

Previously, molecular statics, molecular dynamics and the dimer method have been combined to study the fate of He atoms in the vicinity of dislocations [4,5] and GBs [6,7] in  $\alpha$ -Fe. These results have demonstrated that both substitutional and interstitial

He atoms are trapped at GBs, with binding energies ranging from 0.2 to 0.8 eV and from 0.5 to 2.7 eV, respectively. Molecular dynamics simulations have shown that the diffusion coefficient for He diffusion along an extended defect is expected to depend significantly on the type of extended sink (dislocation or GB). Also, the diffusion mechanisms strongly depend on GB structures and temperatures [6]. It is found that di-He interstitials can migrate rapidly along the  $\Sigma 3$  GB at low temperature, but not along the  $\Sigma 11$  GB. The large variation in density and size of bubbles at different GBs may be correlated with the varying atomistic structures of the GBs, which suggests that the GB's structure is important for the diffusivity of He along GBs. In this paper, the detailed diffusion mechanisms and energy barriers of He interstitials and small He-vacancy clusters in two representative GBs are studied using the dimer method. In parallel, the migrations of vacancies in these GBs are studied using both the dimer method and long-time dynamics simulations to understand their possible contributions to the formation of helium bubbles.

### 2. Simulation methods

The details of the methodology used in the calculations of the atomic arrangement of GBs have been previously described elsewhere [8,9]. The computational cell consists of two parallel sections having different orientations, forming the GB along their interface. The equilibrium structures of the GBs at 0 K are obtained by relaxation using molecular dynamics with an energy quench employing a viscous drag algorithm. Periodic boundary conditions

\* Corresponding author.

E-mail address: [Fei.Gao@pnl.gov](mailto:Fei.Gao@pnl.gov) (F. Gao).

are applied in the directions parallel to the GB plane, whereas a semi-rigid boundary condition is applied in the direction normal to the GB [9]. The two symmetric tilt GBs studied in the present work are  $\Sigma 3\{112\}$   $\theta = 70.53^\circ$  and  $\Sigma 11\{323\}$   $\theta = 50.48^\circ$ , and their corresponding ground-state structures are shown in Kurtz et al. [8]. These two GBs have the same tilt axis ( $\langle 101 \rangle$ ). The  $\Sigma 3\{112\}$  GB has low grain boundary energy and small excess atomic volume, while the  $\Sigma 11\{323\}$  GB has much higher grain boundary energy and larger excess atomic volume. The dimension of the simulation cell is  $33.3 \text{ \AA} \times 36 \text{ \AA} \times 32.4 \text{ \AA}$  consisting of 3120 and 3247 atoms for the  $\Sigma 3$  GB and  $\Sigma 11$  GB, respectively.

Similar to our previous studies [7], the lowest energy configurations of a single He interstitial and a HeV<sub>2</sub> cluster in each GB were determined by raising the lattice temperature to 1000 K, with simulation time up to about 10 ps, and then slowly cooling down to 0 K (see the details below). The possible transitions starting from these stable configurations were systematically searched using the dimer method. The dimer method has been described in detail elsewhere [10,11], and it is different from other widely used saddle point searching algorithms, e.g. the drag and the nudged-elastic band method, in the sense that knowledge of only the initial state is required. In all cases 100 dimer searches were carried out starting from each initial state, and the initial dimer vectors are generated randomly to have non-zero components only on 20–50 atoms around the defect configurations. The end configuration that corresponds to the lowest energy barrier was used for the next set of dimer searches. This approach repeats until the He interstitial and HeV<sub>2</sub> cluster migrate to the positions which are equivalent to their original positions. In addition, long-time dynamics based on the dimer method [12] was employed to investigate the long-time behavior of a single vacancy in the GBs, and to see if a confirmed migration path can be achieved.

The Fe–Fe interaction is described by the potential developed by Ackland et al. [13] based on the Finnis–Sinclair formalism, while the Fe–He potential was fit to ab initio calculations of small He–Fe clusters by Wilson and Johnson [14]. A classical potential developed by Beck [15] was used to describe He–He interactions. The considerations of using this set of potentials have been discussed in detail elsewhere [16]. In the simulations of a vacancy migration, the recently developed Fe–Fe potential by Mendeleev et al. [17] was also used to check the potential-sensitivity of its migration energy and path in both bulk and GBs.

### 3. Results and discussions

The transition states of He interstitials, vacancies and HeV<sub>2</sub> clusters are searched in both the GBs using the dimer method, and 100 dimer searches are carried out for each initial configuration. One of the important parameters in the dimer search is the maximum move distance of the dimer, which has been carefully chosen to obtain a higher success rate of searches (see the details in Henkelman and Jónsson [10]). For example, in a typical run of 100 dimer searches of an initial He configuration in the  $\Sigma 3$  GB, 55 searches converge to saddle points with an energy of 0.46 eV, which corresponds to the migration energy from one site to another (see below). Fifteen searches converge to other saddle points that are not associated with the original minimum energy configuration. Ten searches fail to find saddle points within 500 iterations. The final configuration that is associated with the lowest energy barrier in these initial searches is selected as a starting configuration for the next set of dimer searches, and this approach continues until an equivalent position is found. The highest energy barrier along the lowest energy path is determined to be the corresponding activation energy for migration of a defect or a cluster. Table 1 summarizes the possible migration energies for He intersti-

**Table 1**

Migration energies of He interstitials, vacancies and HeV<sub>2</sub> clusters in both bulk and GBs, along with the migration energies of vacancies calculated using the new Mendeleev potential [17] (as included in the brackets) for comparison.

	$E_m$ (eV)		
	He	V	HeV <sub>2</sub>
$\Sigma 3$	0.46	0.48 (0.38)	0.9
$\Sigma 11$	0.47	0.74 (0.61)	0.92
Bulk	0.08	0.78 (0.64)	1.13

tials, vacancies and HeV<sub>2</sub> clusters in the  $\Sigma 3$  and  $\Sigma 11$  GBs, along with those in the bulk for comparison.

*He interstitial:* The most stable configuration of a He interstitial in the  $\Sigma 3$  GB is shown in Fig. 1(a), as indicated by a small sphere. The He atom is located at the middle of two Fe atoms along the [110] direction, with eight near neighbors, forming an octahedral interstitial. It should be noted that the He atomic position is slightly shifted along the [1-11] direction. Initially, the He atom can migrate from one octahedral position below the GB plane to a similar position above the GB plane along the [-1-1] direction, as indicated by one of the arrows, overcoming an energy barrier of 0.46 eV. It is found that the He atom can further migrate to an equivalent position below the GB plane with the same energy along the [1-1-1] direction, but in a different atomic row, which results in the net diffusion of the He atom along the [1-11] direction. The corresponding path is denoted as path A. If the He migrates to a row above the GB plane along the [-111] direction, and then migrates to a different location in its initial row along the [-1-1-1] direction, the migration of the He atom leads to its net diffusion along the [110] direction, which is denoted as path B. These two paths have the same migration energy and are equivalent, which may be associated with the typical atomic structure of the  $\Sigma 3$  GB. It is clear from these dimer searches that the He atom can migrate either along the [1-11] direction or along the [110] direction with the same activation energy, which results in its two-dimensional migration within the GB plane. Previously, a molecular dynamics method was employed to study the diffusion mechanism of a He interstitial in the  $\Sigma 3$  GB [7], and the simulations revealed that the He atom migrates two-dimensionally at low temperature and three-dimensionally at higher temperatures. The present dimer results are in excellent agreement with the previous MD simulations, and they now provide a physical explanation for the observed phenomena.

Fig. 1(b) shows the initial position of the He atom in the  $\Sigma 11$  GB and possible migration paths. The most stable configuration of the He atom is located at the middle site of two planes consisting of three Fe atoms, respectively, as indicated by a small sphere. This position is equivalent to the tetrahedral position in a perfect crystal of  $\alpha$ -Fe, but it has more nearest-neighbors (total six, rather than four). The dimer searches indicate that the He atom can migrate from the tetrahedral position below the GB plane to a similar position above the GB plane, and this movement leads to the He atom diffusion along the [-113] direction, as indicated by the arrows. This path is the lowest energy path, and the corresponding activation energy is about 0.47 eV, which is similar to that for He in the  $\Sigma 3$  GB. Also, the dimer searches reveal other possible transition states, but with much higher energies. These results suggest that the He atom migrates one-dimensionally along the [-113] direction, but its path is zigzag along the interface in the same plane. The present dimer results are in good agreement with the previous MD studies [7]. The MD simulations suggest that the He interstitial is strongly bound to the middle plane on which the initial starting position of the He interstitial is allocated, and it can only move in the spaces between the three planes. However, it should be noted that the migration energies of He atoms given by the MD

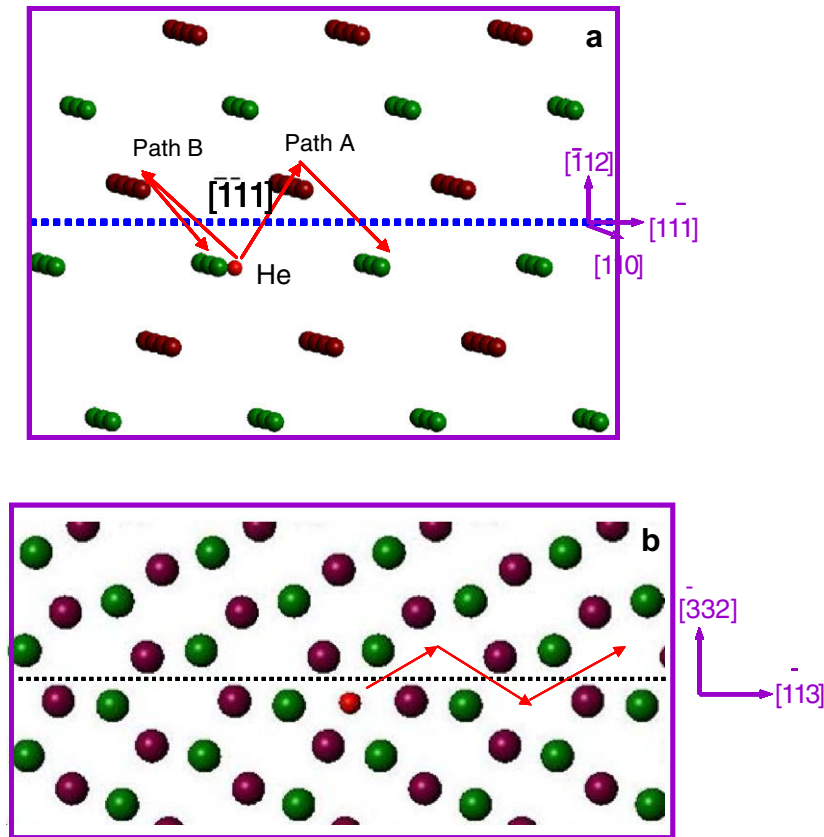


Fig. 1. Possible migration paths of a He interstitial in (a) the  $\Sigma 3$  GB and (b) the  $\Sigma 11$  GB, where a small sphere represents the He atom and arrows indicate possible paths.

simulations are smaller than those by the static calculations, which is expected. The difference between the previous simulations and the present calculations may be due to the fact that He atoms migrate one- or two-dimensionally, and the analysis of mean square displacements, even with an advanced method of decomposing the single trajectory into a set of shorter independent segments with equal duration, can lead to a large error (up to 40%).

**Vacancy:** One of the components controlling He bubble nucleation and growth is the mobility of vacancies in both bulk and GBs. It is well known that a vacancy in the bulk Fe migrates three-dimensionally, with an activation energy of 0.78 eV (Ackland potential) or 0.64 eV (Mendelev potential). Both He atoms and vacancies can be deeply trapped by dislocations and GBs, and the fundamental understanding of their migrations within dislocations and GBs is important for multi-scale computer simulation of microstructural evolution under radiation conditions. The results described here are mainly obtained using the Ackland Fe potential, but their sensitivities have been carefully checked using the Mendelev Fe potential (see below). The dimer searches obtain the lowest vacancy migration energy to be 0.48 eV in the  $\Sigma 3$  GB, which is much smaller than that in the bulk. The surprising result is that the vacancy migrates one-dimensionally along the  $\Sigma 3$  GB, as demonstrated in Fig. 2(a), where the arrows indicate possible paths. To change its migration behavior from one atomic row to another requires much higher energy ( $\sim 0.9$  eV). A long-time dynamics simulation has also been carried out to study the vacancy migration, and it is found that the vacancy moves forwards and backwards along the  $[1\bar{1}1]$  direction. This confirms that the vacancy migrates only one-dimensionally with a similar energy to that of a He interstitial in the  $\Sigma 3$  GB.

Fig. 2(b) shows the possible mechanisms for a vacancy to migrate in the  $\Sigma 11$  GB, and its path is a zigzag path along the inter-

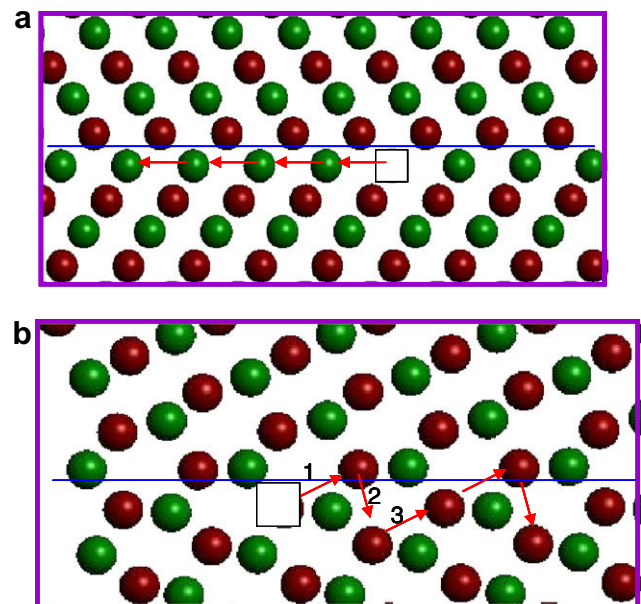


Fig. 2. Possible paths of a trapped vacancy in (a) the  $\Sigma 3$  GB and the  $\Sigma 11$  GB, where the white squares represent vacancies and arrows indicate their movements along the GBs.

face, with strong bonding to the interface. As can be seen, several directional changes are required for its migration, but these zigzag paths eventually lead to its one-dimensional migration along the interface, a similar behavior to that in the  $\Sigma 3$  GB. The corresponding energies are 0.73, 0.74 and 0.41 eV for paths 1, 2 and 3,

respectively. The highest energy barrier corresponds to the migration energy of a vacancy in the  $\Sigma 11$  GB. One of the interesting results is that the vacancy migrates within a plane perpendicular to the interface, and the migration out of the plane requires much higher energy ( $\sim 0.77$  and  $0.9$  eV within the  $\Sigma 3$  and  $\Sigma 11$  GBs, respectively). These results suggest that the vacancies may migrate one-dimensionally at low temperatures and two-dimensionally at higher temperatures.

We have also used the new Fe potential recently developed by Mendeleev et al. [17] to study the vacancy migration in both GBs, and the results are also listed in Table 1, as included in the brackets. The migration energies obtained with this new potential are generally smaller than those given by the Ackland potential in the bulk and GBs. However, the migration mechanisms of the vacancies are very similar to those observed using the Ackland potential, i.e. the vacancy migrates one-dimensionally along the  $[1-11]$  direction in the  $\Sigma 3$  GB, whereas its path is a zigzag path in the  $\Sigma 11$  GB, with one-dimensional behavior along the  $[-113]$  direction. While calculations using other Fe potentials, such as angle-dependent and bond-order potentials, and by ab initio methods may alter the migration energies slightly, it is likely that the migration mechanisms observed in the present study will not change significantly because the migration mechanisms are strongly related to the GB structures. It should also be noted that use of different potentials may lead to somewhat different structures for the two grain boundaries considered here. In the present work, the ground-state structures for the  $\Sigma 3\{112\}$  and  $\Sigma 11\{323\}$  GBs were also modeled using the Mendeleev potential, and the atomic arrangements within these GBs are essentially similar to those given by the Ackland potential, which demonstrates that at least for these systems the effects of interatomic potentials on the GB structures is small.

**HeV<sub>2</sub> cluster:** It has been proposed that the migration of substitutional helium by the vacancy mechanism is governed by the migration of the HeV<sub>2</sub> complex [18]. The most stable configuration for a HeV<sub>2</sub> complex in the GBs is found to be two first neighbor vacancies, with a He atom located between them, as shown in Fig. 3(a). This configuration is slightly different from the most stable configuration of the HeV<sub>2</sub> cluster in the bulk, where the He atom is substitutional He, but slightly displaced from one vacancy along the line between the two vacancies. To understand the

migration of a HeV<sub>2</sub> cluster within GBs, the dimer searches of transition states were first carried out to study its migration in the bulk. The results show that there exist a number of possible transition states. The lowest transition state corresponds to the He jumping from one vacancy to the other with an activation energy of  $0.02$  eV for first neighbor vacancies, but this energy increases to  $0.66$  eV for second neighbor vacancies. It is found that the migration of the HeV<sub>2</sub> cluster is dominated by the vacancy migration, rather than by the He atom, i.e. it is a vacancy mechanism. The migration energy is determined to be about  $1.13$  eV. Fu and Willaime [18] studied the migration of a HeV<sub>2</sub> cluster in the bulk using ab initio methods, and they found that the HeV<sub>2</sub> cluster can migrate as a unit over appreciable distance via substitutional He-vacancy mechanisms, with an activation energy of  $1.17$  eV. The mechanisms and migration energy obtained in the present study are in excellent agreement with their results.

Fig. 3 shows the migration mechanisms of a HeV<sub>2</sub> cluster in the  $\Sigma 3$  GB, and its path is a rotational path within the interface. Starting with the stable configuration, the He atom diffuses into the nearest vacancy site above the GB plane, and becomes a substitutional He. At the same time, an Fe atom close to one of two vacancies below the GB plane diffuses into this vacancy site, resulting in a configuration where the He atom and the vacancy are in second neighbor positions, as exhibited in Fig. 3(b). The arrows in Fig. 3(a) indicate the movements of the He atoms and vacancies, and it should be noted that the migration behavior of the HeV<sub>2</sub> cluster shows a collective motion. However, these defects are strongly bound to the interface, and the possible dissociation from the interface requires much higher energy. The further diffusion of a Fe atom above the GB plane to the vacancy and of the He atom to a nearest-neighbor site lead to the formation of a configuration similar to the initial configuration, but with different direction. This collective motion is indicated by the arrows in Fig. 3(b). There are two possible migration paths for the configuration in Fig. 3(c), one back to its original position in Fig. 3(a) and another resulting in its migration along the  $[-11-1]$  direction. Similar to the migration of a vacancy, these collective motions eventually lead to the one-dimensional migration along the interface, and the corresponding migration energy is determined to be  $0.9$  eV. It should be emphasized that these collective motions occur within a plane perpendicular to the interface, and the out-of-plane migration of the HeV<sub>2</sub>

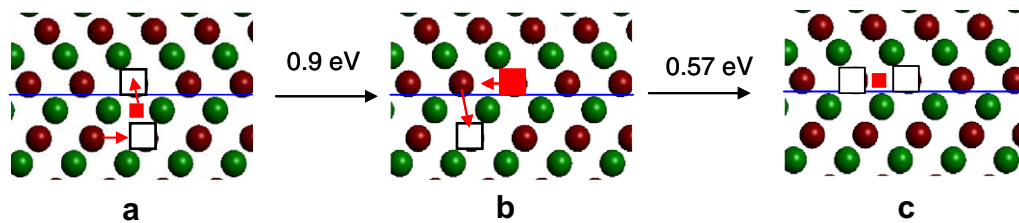


**Fig. 3.** Migration mechanism of a HeV<sub>2</sub> cluster in the  $\Sigma 3$  GB, where the arrows indicate the collective motion of Fe and He atoms, resulting in its one-dimensional migration along the GB. The migration energy is determined to be  $0.9$  eV.

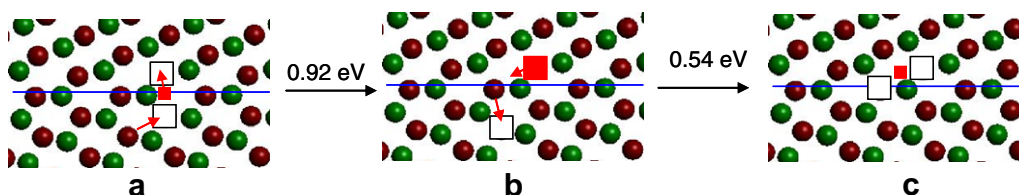


**Fig. 4.** Migration mechanism of a HeV<sub>2</sub> cluster in the  $\Sigma 11$  GB, where the arrows indicate the collective motion of Fe and He atoms, resulting in the cluster's one-dimensional migration along the GB. The migration energy is determined to be  $0.92$  eV.

cluster is not observed, or it may require much higher energy. A similar behavior of the HeV<sub>2</sub> cluster in the  $\Sigma 11$  GB is observed, as shown in Fig. 4, and its migration energy is about 0.92 eV. It is noted that the migration energy of a HeV<sub>2</sub> in the GBs is similar to that in the bulk, but the migration mechanisms are completely different. In the bulk, the HeV<sub>2</sub> cluster can migrate three-dimensionally, while it migrates only one-dimensionally via the substitutional He-vacancy migration mechanism within the GBs. The one-dimensional behavior of He interstitials, vacancies and HeV<sub>2</sub> clusters may play important roles in the nucleation and growth of helium bubbles in the GBs.

#### 4. Conclusions

The possible migration paths and mechanisms of vacancies, He interstitials and He-vacancy (He/V) clusters at  $\Sigma 11\langle 110 \rangle \{323\}$  and  $\Sigma 3\langle 110 \rangle \{111\}$  GBs are studied by combining the dimer saddle point searches and long-time dynamics in  $\alpha$ -Fe. In contrast to the three-dimensional migration behavior of vacancies, they migrate one-dimensionally along specific directions, with migration energies less than that in bulk Fe. Long-time dynamics simulations of diffusion pathways reveal that vacancies migrate one-dimensionally along close-packed rows in the  $\Sigma 3$  GB and in zigzag paths within the  $\Sigma 11$  GB. He interstitials can diffuse along the GBs with migration energies of 0.4–0.5 eV, similar to those of individual vacancies at the GBs. There are two equivalent paths for a He interstitial within the  $\Sigma 3$  GB plane, leading to its two-dimensional migration, but there is only one possible path in the  $\Sigma 11$  GB. These results provide a detailed explanation of why the He atom migrates two-dimensionally at low temperatures and three-dimensionally at higher temperatures in the  $\Sigma 3$  GB, but only one-dimensionally in the  $\Sigma 11$  GB, as observed previously in the long-time MD simu-

lations. The migration energy of a He-divacancy cluster in the GBs using the dimer method is determined to be about 0.9 eV, and the corresponding migration mechanism shows that its path is a rotational path within the GBs, but its collective motion exhibits one-dimensional migration along the GBs.

#### Acknowledgments

This research is supported by the US Department of Energy, Office of Fusion Energy Sciences under Contract DE-AC06-76RLO 1830.

#### References

- [1] K. Farrell, P.J. Maziasz, E.H. Lee, L.K. Mansur, *Radiat. Eff. Defect S.* 78 (1983) 277.
- [2] S.J. Zinkle, N.M. Ghoniem, *Fusion Eng. Des.* 51&52 (2000) 55.
- [3] E.E. Bloom, J.T. Busby, C.E. Duty, P.J. Maziasz, et al., *J. Nucl. Mater.* 367–370 (2007) 1.
- [4] R.J. Kurtz, H.L. Heinisch, *J. Nucl. Mater.* 329–333 (2004) 1199.
- [5] H.L. Heinisch, F. Gao, R.J. Kurtz, *J. Nucl. Mater.* 367–370 (2007) 311.
- [6] F. Gao, H.L. Heinisch, R.J. Kurtz, *J. Nucl. Mater.* 351 (2006) 133.
- [7] F. Gao, H.L. Heinisch, R.J. Kurtz, *J. Nucl. Mater.* 367–370 (2007) 446.
- [8] R.J. Kurtz, R.G. Hoagland, J.P. Hirth, *Philos. Mag. A* 79 (1999) 665.
- [9] R.J. Kurtz, R.G. Hoagland, J.P. Hirth, *Philos. Mag. A* 79 (1999) 683.
- [10] G. Henkelman, H. Jónsson, *J. Chem. Phys.* 111 (1999) 7010.
- [11] F. Gao, G. Henkelman, W.J. Weber, L.R. Corrales, H. Jónsson, *Nucl. Instr. and Meth. B* 202 (2003) 1.
- [12] G. Henkelman, H. Jónsson, *J. Chem. Phys.* 115 (2001) 9657.
- [13] G.J. Ackland, D.J. Bacon, A.F. Calder, T. Harry, *Philos. Mag. A* 75 (1997) 713.
- [14] W.D. Wilson, R.D. Johnson, *Rare gases in metals*, in: P.C. Gehlen, J.R. Beeler Jr., R.I. Jaffee (Eds.), *Interatomic Potentials and Simulation of Lattice Defects*, Plenum, 1972, p. 375.
- [15] D.E. Beck, *Mol. Phys.* 14 (1968) 311.
- [16] H.L. Heinisch, F. Gao, R.J. Kurtz, E.A. Le, *J. Nucl. Mater.* 351 (2006) 141.
- [17] M.I. Mendeleev, S. Han, D.J. Srolovitz, G.J. Ackland, D.Y. Sun, M. Asta, *Phil. Mag.* 83 (2004) 3977.
- [18] C.C. Fu, F. Willaime, *Phys. Rev. B* 72 (2005) 064117.